

## P4-2

Investigation of  $(\text{HfO}_2)_x(\text{Al}_2\text{O}_3)_{1-x}$  on (100) Si by XPS – energy gap and band alignmentH. Y. Yu<sup>1</sup>, M. F. Li<sup>1</sup>, D.L. Kwong<sup>2</sup>, B.J.Cho<sup>1</sup>, J.S.Pan<sup>3</sup>, C.H.Ang<sup>4</sup> and J.Z. Zheng<sup>4</sup><sup>1</sup> Silicon Nano Device Lab, ECE Department, National University of Singapore, Singapore 119260.Tel: 65-8742559, Fax: 65-7791103, Email: [elelimf@nus.edu.sg](mailto:elelimf@nus.edu.sg)<sup>2</sup> Dept. Electrical and Computer Engineering, University of Texas at Austin, Austin, TX 78712, USA.<sup>3</sup> Institute of Materials Research & Engineering, 3 Research Link, Singapore 117602<sup>4</sup> Chartered Semiconductor Manufacturing Ltd. Singapore 738406

## 1. Introduction

$\text{HfO}_2$  has emerged as one of the most promising high-k candidates due to its high dielectric constant, large energy gap, and its compatibility with conventional CMOS process [1,2]. However, it may suffer re-crystallization at high temperature during post deposition annealing (PDA), which in turn, may induce higher leakage current and severe boron penetration issues. On the other hand,  $\text{Al}_2\text{O}_3$  films grown directly on Si were reported to remain amorphous up to 1000°C [3]. Recently Al has been proposed to alloy  $\text{HfO}_2$  to raise the dielectric crystallization temperature, and encouraging results were demonstrated [4]. In this work, the energy gap  $E_g$  of  $(\text{HfO}_2)_x(\text{Al}_2\text{O}_3)_{1-x}$ , the valence band offset  $\Delta E_v$  and the conduction band offset  $\Delta E_c$  between  $(\text{HfO}_2)_x(\text{Al}_2\text{O}_3)_{1-x}$  and the Si as functions of  $x$  are obtained based on XPS measurement. These information are of vital importance in assessing  $(\text{HfO}_2)_x(\text{Al}_2\text{O}_3)_{1-x}$  as the most promising high k gate dielectric in future CMOS device technology.

## 2. The Experiments

A total of five  $(\text{HfO}_2)_x(\text{Al}_2\text{O}_3)_{1-x}$  samples of various  $x$  values were prepared by atomic layer deposition (ALD), with low-doped p-type Si(100) wafers as substrates ( $n_a \sim 10^{15} \text{ cm}^{-3}$ ), at 300 °C. The thicknesses of the  $(\text{HfO}_2)_x(\text{Al}_2\text{O}_3)_{1-x}$  films are ~20 nm. The *ex-situ* XPS measurements were carried out using a VG ESCALAB 220i-XL system, equipped with a monochromatize Al-K $\alpha$  source for excitation of photoelectrons. All of the high-resolution scans were taken at a photoelectron take-off angle of 90° and a pass energy of 20 eV. Under such configurations, the full width at half maximum (FWHM) of Si 2p core level recorded from H-terminated Si surface was measured as ~0.45 eV, which gives an indication of the instrument energy resolution. Al 2p, Hf 4f, C 1s, O 1s, valence band maximum (VBM), and O 1s energy loss spectra were measured and analyzed. The intensities for all the XPS spectra have been normalized for comparison and all of the spectra are calibrated against C 1s peak (285.0 eV).

## 3. Results and Discussion

The chemical compositions of various  $(\text{HfO}_2)_x(\text{Al}_2\text{O}_3)_{1-x}$  samples can be determined by the intensities of the XPS lines. The five samples are denoted as HAO-1 to HAO-5 respectively, and their corresponding elemental compositions as well as the values of  $x$  are given in Table-I. All the samples show good stoichiometry and trace amount of carbon (~ 5 at. %) are detected from all of the samples surfaces.

XPS spectra for Hf 4f, Al 2p, and O 1s core levels are shown as in Fig. 1 – 3. It is observed that all the core level peak positions of Hf 4f, Al 2p, and O 1s experience a shift to higher

binding energy with the increase of Al concentration in  $(\text{HfO}_2)_x(\text{Al}_2\text{O}_3)_{1-x}$  system. The above shift is due to the fact that Hf is a more ionic cation than Al in  $(\text{HfO}_2)_x(\text{Al}_2\text{O}_3)_{1-x}$ , and thus the charge transfer contribution changes with the increase of Al composition [5,6]. For the O 1s core level spectra (the solid lines), a curve-fitting method (the dashed lines) is applied to analyze the variation in O 1s spectra shape. For the samples HAO-2, HAO-3, and HAO-4, three peaks can be clearly resolved. The peak located at ~ 530.5 eV is attributed to Hf-O bonds, and another peak at ~ 531.2 eV to Al-O bonds. It is obvious that Al-O components increase with Al in  $(\text{HfO}_2)_x(\text{Al}_2\text{O}_3)_{1-x}$ . The shoulder at ~ 532.3 eV is generally interpreted as due to C-O bonds [7]. We observe this shoulder decreases with the decrease of Hf component. Hf 4s line is also located around this energy [8]. Thus, it is suggested that both of the above-indicated sources contribute to the peak at ~532.3 eV.

Fig. 4 shows the O 1s energy-loss spectra, which are caused by the outgoing photoelectrons suffering inelastic losses to collective oscillations (plasmon) and single particle excitations.  $E_g$  values for the dielectric materials can be determined by the onsets of energy loss from the spectra [9,10]. By this mean,  $E_g$  for  $\text{HfO}_2$  is measured as  $5.25 \pm 0.10$  eV, and for  $\text{Al}_2\text{O}_3$  as  $6.52 \pm 0.10$  eV.  $E_g$  of  $\text{Al}_2\text{O}_3$  is consistent with those reported by Itokawa et al ( $6.55 \pm 0.05$  eV) [10] and Bender et al ( $6.7 \pm 0.2$  eV) [11]. From this figure, a linear change of energy gap value with  $x$  in the  $(\text{HfO}_2)_x(\text{Al}_2\text{O}_3)_{1-x}$  system is observed.

The determination of  $\Delta E_v$  was performed by measuring the difference of valence band maximum (VBM) between the  $(\text{HfO}_2)_x(\text{Al}_2\text{O}_3)_{1-x}$  grown on p-Si(100) and the H-terminated p-Si(100) substrate, as demonstrated in Fig. 5. The VBM for each sample is defined by extrapolating the leading edge of valence band spectrum to the baseline (the cross points in Fig. 5) from its specific spectrum [9].

Hence  $\Delta E_v$  values of  $3.03 \pm 0.05$  eV and  $2.22 \pm 0.05$  eV are obtained for  $\text{Al}_2\text{O}_3$  and  $\text{HfO}_2$ .  $\Delta E_v$  of  $\text{Al}_2\text{O}_3$  is consistent with the value  $2.9 \pm 0.2$  eV reported by Bender et al [11]. A gradual change in the valence band density of states is also observed from sample HAO-1 to HAO-5.

Table I. Elemental composition and the  $\text{HfO}_2$  mole fraction value  $x$  of various  $(\text{HfO}_2)_x(\text{Al}_2\text{O}_3)_{1-x}$  samples estimated by XPS.

	HAO-1 ( $\text{HfO}_2$ )	HAO-2	HAO-3	HAO-4	HAO-5 ( $\text{Al}_2\text{O}_3$ )
Hf at. %	33.9%	25.8%	18.4%	9.6%	0
Al at. %	0	9.2%	18.2%	27.7%	39.8%
O at. %	66.1%	65%	63.4%	62.7%	60.2%
x value	1	~0.85	~0.67	~0.41	0

With knowledge of  $E_g$  of Si (1.12 eV),  $\Delta E_c$  for  $\text{HfO}_2$  is calculated as  $1.91 \pm 0.15$  eV, and for  $\text{Al}_2\text{O}_3$  as  $2.37 \pm 0.15$  eV. Afanas'ev et al. reported  $3.23 \pm 0.08$  eV for the (100) Si valence band to  $\text{Al}_2\text{O}_3$  conduction band offset, measured by internal photoemission [12]. Considering  $E_g$  of Si, the Si to  $\text{Al}_2\text{O}_3$  conduction band offset  $\Delta E_c$  is calculated to be  $2.11 \pm 0.08$  eV, which in turn, is in reasonable agreement with our XPS result. Fig. 6 – 7 depict the schematic energy band alignment of  $\text{HfO}_2$  and  $\text{Al}_2\text{O}_3$  on Si based on XPS. Note both  $\Delta E_c$  and  $\Delta E_v$  for  $\text{Al}_2\text{O}_3$  are greater than those for  $\text{HfO}_2$ .

The  $E_g$ ,  $\Delta E_v$ , and  $\Delta E_c$  values obtained by XPS measurements for samples HAO-1 to HAO-5 are plotted in Fig. 8. By linear least square fit, the following equations are obtained:

$$E_g = 6.52 - 1.27x \text{ (eV)}; \quad (1a)$$

$$\Delta E_v = 3.03 - 0.81x \text{ (eV)}; \quad (1b)$$

$$\Delta E_c = 2.37 - 0.46x \text{ (eV)}. \quad (1c)$$

where  $x$  stands for the mole fraction of  $\text{HfO}_2$  in  $(\text{HfO}_2)_x(\text{Al}_2\text{O}_3)_{1-x}$ , as is clearly demonstrated in table I. Accordingly, the electrical properties of  $(\text{HfO}_2)_x(\text{Al}_2\text{O}_3)_{1-x}$  gate dielectrics can be tuned by simply changing the  $\text{HfO}_2$  mole fraction while keeping the stoichiometry of the materials.

#### 4. Conclusion

High-resolution XPS measurements were performed to investigate  $E_g$  and  $\Delta E_v$  of  $(\text{HfO}_2)_x(\text{Al}_2\text{O}_3)_{1-x}$  high-k materials.

Al 2p, Hf 4f, O 1s core levels spectra, valence band spectra, and O 1s energy loss spectra all show continuous changes with the variation of  $\text{HfO}_2$  mole fraction  $x$  in  $(\text{HfO}_2)_x(\text{Al}_2\text{O}_3)_{1-x}$ .  $E_g$ ,  $\Delta E_v$ , and  $\Delta E_c$  values for  $(\text{HfO}_2)_x(\text{Al}_2\text{O}_3)_{1-x}$  on Si (100) are determined and can be expressed by  $6.52 - 1.27x$  (eV),  $3.03 - 0.81x$  (eV), and  $2.37 - 0.46x$  (eV) respectively.

This work was supported by the Singapore NSTB/EMT/TP/00/001.2 grant. We thank for by GENUS Inc. USA for the deposition of  $(\text{HfO}_2)_x(\text{Al}_2\text{O}_3)_{1-x}$  films.

#### References

- [1] S. J. Lee et al., IEDM Tech. Dig., p. 31 (2000)
- [2] L. Kang et al., IEDM Tech. Dig., p. 35 (2000)
- [3] A. Chin et al., Symp. VLSI Tech. Dig., p135 (1999)
- [4] W. Zhu, et al. IEDM Tech. Dig., p. 20.4.1 (2001)
- [5] M. J. Guittet, et al. Phys. Rev. B, **63**, 125117 (2001)
- [6] G. Lucovsky, International Workshop on Gate Isolation, (IWGI), Tokyo (2001)
- [7] H. Y. Yu, et al. Appl. Phys. Lett., **78**, 2595 (2001)
- [8] J. F. Moulder, et al., Handbook of X-ray Photoelectron Spectroscopy, 2<sup>nd</sup> ed. Physical Electronics, Eden Prairie, (1992)
- [9] F. G. Bell, L. Ley, Phys. Rev. B, **37**, 8383 (1988)
- [10] H. Itokawa, et al. Extended Abstracts of SSDM, p. 158 (1999)
- [11] H. Bender, et al. IWGI, Tokyo (2001)
- [12] V. V. Afanas'ev, et al. Appl. Phys. Lett., **78**, 3073 (2001)

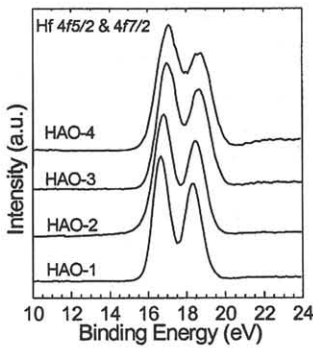


Fig.1 XPS spectra for Hf 4f core levels taken from various  $(\text{HfO}_2)_x(\text{Al}_2\text{O}_3)_{1-x}$  samples.

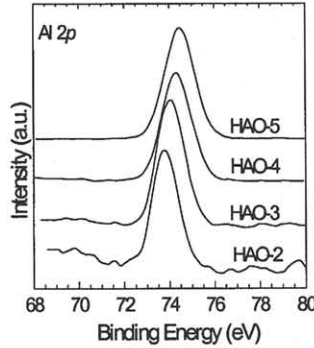


Fig.2 XPS spectra for Al 2p core levels taken from various  $(\text{HfO}_2)_x(\text{Al}_2\text{O}_3)_{1-x}$  samples.

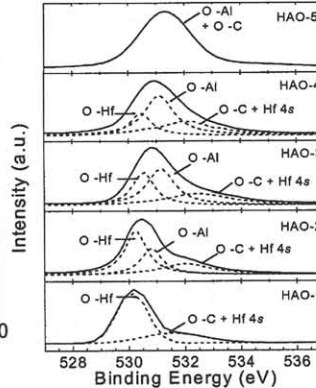


Fig.3 XPS spectra for O 1s core levels taken from various  $(\text{HfO}_2)_x(\text{Al}_2\text{O}_3)_{1-x}$  samples.

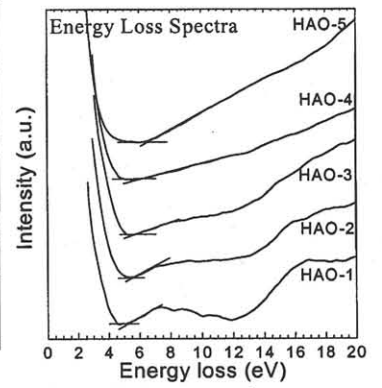


Fig.4: O 1s energy-loss spectra for various  $(\text{HfO}_2)_x(\text{Al}_2\text{O}_3)_{1-x}$  samples.

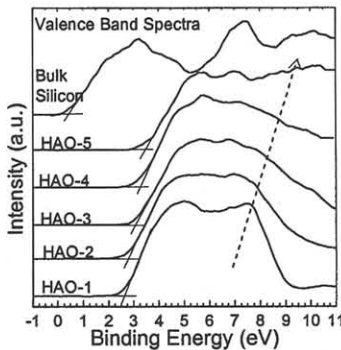


Fig.5: XPS VB spectra from various  $(\text{HfO}_2)_x(\text{Al}_2\text{O}_3)_{1-x}$  grown on (100)Si and H-terminated (100)Si. Dashed arrow: the gradual change in the VB-DOS from sample HAO-1 to HAO-5.

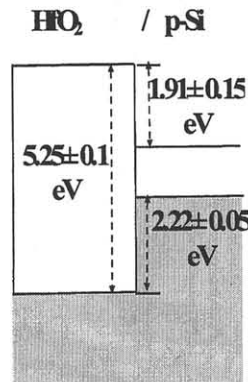


Fig.6: Schematic energy band alignment of  $\text{HfO}_2$  on (100) Si substrate based on XPS measurements

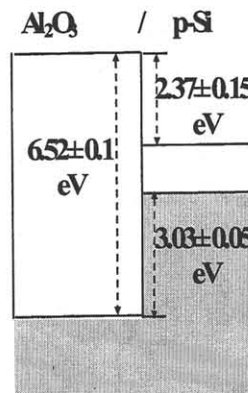


Fig.7: Schematic energy band alignment of  $\text{Al}_2\text{O}_3$  on (100) Si substrate based on XPS measurements

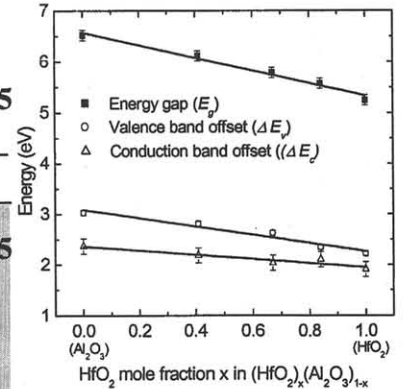


Fig.8: Dependence of  $E_g$ ,  $\Delta E_v$ , and  $\Delta E_c$  for  $(\text{HfO}_2)_x(\text{Al}_2\text{O}_3)_{1-x}$  on  $\text{HfO}_2$  mole fraction  $x$ . The solid lines are obtained by linear least square fits of the data points.